Diamond & Related Materials 19 (2010) 748–751

Contents lists available at ScienceDirect

Diamond & Related Materials

journal homepage: www.elsevier.com/locate/diamond

The influence of nanoscale defects on the fracture of multi-walled carbon nanotubes under tensile loading

Go Yamamoto [a,b,*], Ji Won Suk [c], Jinho An [c], Richard D. Piner [c], Toshiyuki Hashida [b], Toshiyuki Takagi [a], Rodney S. Ruoff [c]

[a] Institute of Fluid Science, Tohoku University, Sendai 980-8577, Japan
[b] Fracture and Reliability Research Institute, Tohoku University, Sendai 980-8579, Japan
[c] Department of Mechanical Engineering and the Texas Materials Institute, University of Texas, Austin, Texas 78712, USA

ARTICLE INFO

Available online 1 February 2010

Keywords:
Nanotubes
Nanostructures
Defects
Mechanical properties

ABSTRACT

We report the mechanical behavior of a unique type of multi-walled carbon nanotube (MWCNT) and an acid-treated version of this MWCNT type that have nanoscale defects on their surfaces from the acid treatment. These defects, from scanning electron microscope (SEM) and transmission electron microscope (TEM) imaging have a 'channel-like' appearance, as if a ring of material was cut away from the MWCNT around the circumference. The mechanical properties of individual MWCNTs have been experimentally shown to strongly depend on their structure and structural disorder can drastically reduce the mechanical properties. Tensile-loading experiments using a nanomanipulator tool operated inside a SEM revealed that the tensile strengths of 10 pristine MWCNTs ranged from ~2 to ~48 GPa (mean 20 GPa). For 10 acid-treated MWCNTs with channel-like defects, tensile strengths ranged from ~1 to ~18 GPa (mean 6 GPa, thus roughly 70% lower than those of the pristine MWCNTs). Microstructural observations revealed that the fracture of the acid-treated MWCNTs occurred at a channel-like defect region in 8 of the 10 samples. This indicates that the channel-like defects associated with the acid etching are typically going to be the weakest points in the acid-treated MWCNT structure and that stress concentration is present at the defect region.

1. Introduction

Experimental and theoretical results regarding the mechanical properties of carbon nanotubes (CNTs) suggest that they hold great promise as a reinforcing phase in new kinds of composite materials [1–8]. Quantum mechanics calculations predict that defect-free CNTs possess tensile strength in excess of 100 GPa, that they have a Young's modulus close to 1100 GPa (with an assumed shell thickness of 0.34 nm) and that they are calculated to have a fracture strain in the range of 15–30% [9–14]. However, experimental measurements to date [15–18] except for one report [19] have observed lower values for the expected fracture strength and failure strain. Calculations have suggested that one- or two-atom vacancy defects on the CNT can reduce failure stresses by as much as ~26% and markedly reduce failure strain. Furthermore, larger holes can greatly reduce strength, and this provided an explanation for some discrepancies between theory and experiment [14].

Recently, an unusual type of multi-walled carbon nanotube (MWCNT) synthesized with a catalytic chemical vapor deposition (CCVD) method followed by a series of high temperature annealing steps culminating with annealing at 2600 °C, was reported [20,21]. This type of MWCNT has highly crystalline layers and is partially facetted in its cross-section [20]. The structure of these MWCNTs suggests they might have interesting mechanical properties and fracture behavior. In addition, we recently demonstrated that the addition of this type of MWCNT (but with nanoscale defects deliberately created on the surface of the MWCNTs though an acid treatment) to alumina ceramics, results in 27% and 25% increases in bending strength and fracture toughness, respectively [7]. This suggests enhanced stress transfer from the matrix to the MWCNTs through mechanical interlocks between the alumina matrix and the acid-treated modified MWCNTs [7].

Defects have already received considerable attention [7,14,22,23], in part because they can be readily induced by either 'purification' step(s) during processing or by surface modification of CNTs. However, direct measurements of the tensile response of CNTs having nanoscale defects deliberately induced on their surface have heretofore not yet been reported.

2. Experimental

The MWCNT material (acquired from Nano Carbon Technologies Corporation; Tokyo, Japan) was synthesized by a catalytic chemical vapor deposition (CCVD) method followed by high temperature annealing [20].

* Corresponding author. Institute of Fluid Science, Tohoku University, 6-6-11-707 Aza-Aoba, Aramaki, Aobaku, Sendai 980-8579, Japan. Tel.: +81 22 795 7524; fax: +81 22 795 4311.
E-mail address: gyamamoto@rift.mech.tohoku.ac.jp (G. Yamamoto).

0925-9635/$ – see front matter © 2010 Published by Elsevier B.V.
doi:10.1016/j.diamond.2010.01.045

The typical diameter and length of the pristine MWCNTs from scanning electron microscopy (SEM, Hitachi S-4300) and transmission electron microscopy (TEM, Hitachi HF-2000) measurements ranged from 33 to 124 nm (average: 70 nm) and 1.1 to 22.5 μm (average: 8.7 μm), respectively. A subset of the pristine MWCNTs was refluxed in a 3:1 (volume ratio) concentrated H_2SO_4:HNO_3 mixture at 70 °C for 2 h, washed thoroughly with distilled water to be acid-free, and then finally dried in an air oven at 60 °C [7].

Tensile tests of individual MWCNTs were performed with a nanomanipulator [15,24] inside the vacuum chamber of a SEM (FEI Quanta 600 FEG). An AFM cantilever (NSC12/without Al/50, nominal force constant 0.3 N/m; Silicon-MDT, Ltd.) was mounted at the end of a piezoelectric bender (Noliac, ceramic plate bender CMBP01) on the X–Y linear motion stage, and a W wire was mounted on an opposing Z linear motion stage. MWCNT powder was dispersed in ethanol with the aid of a magnetic stirrer, and then filtered. The resulting MWCNT paper was torn apart by hand, which caused individual MWCNTs to project from the torn edge. Each MWCNT was extracted from the edge, and then was clamped first onto a cantilever tip and then onto an opposing W wire by electron beam induced deposition (EBID) of a carbonaceous material [25]. The cantilevers serve as force-sensing elements and their force constants were calibrated *in situ* prior to the tensile test using the resonance method developed by Sader et al. [26]. In brief, for the case of a rectangular cantilever, the force constant (k) is given by $k = M_e \rho_c bhL\omega_{vac}^2$, where ω_{vac} is the fundamental radial resonat frequency of the cantilever in vacuum, h, b, and L are the thickness, width, and length of the cantulever, respectively, ρ_c is the density of the cantilever ($=2.33$ Mg/m^3), and M_e is the normalized effective mass which takes the value $M_e = 0.2427$ for $L/b > 5$ [27]. We measured ω_{vac}, h, b, and L of each cantilever in the SEM and used the measured, not the nominal provided, values to calculate k. The h, b, and L are determined by counting the number of pixels in the acquired SEM images. The applied force is calculated from the angle of deflection at the cantilever tip, and the nanotube elongation is determined by counting the number of pixels in the acquired SEM images [24]. The deflection (δ) and angle of deflection (θ) at the cantilever tip are given by $\delta = PL^3/3EI$ and $\theta = PL^2/2EI$, where P is the load applied at the cantilever tip, L is the cantilever length, E is the elastic modulus and I is the moment of inertia of the cantilever [24]. Thus, the deflection at the cantilever tip can be represented by the angle of deflection with the following relationship: $\delta = 2\theta L/3$ [24]. A crosshead speed (i.e., movement rate of the cantilever) of about 0.1 μm/s was applied for the tensile tests. Each MWCNT diameter was measured at magnification ~100,000 in the SEM. Comparison of images of 6 pristine MWCNTs acquired by TEM (Jeol 2010F) and SEM revealed that the differences in the diameters measured by each method was less than ±3 nm; this shows that the diameters obtained by SEM imaging are reliable. For the 20 CNTs tested and reported here, SEM imaging provided the dimensions.

3. Results and discussion

Fig. 1 shows TEM images of the pristine and acid-treated MWCNTs. TEM observations revealed that the pristine MWCNTs have a 'crystalline' multi-walled structure with a narrow central channel (Fig. 1a). Similar observations have been made by others on this type of MWCNT [20]. The acid treatment introduced nanoscale defects with a 10–20 nm depth on the surface of the MWCNTs (Fig. 1b) [7]. The defects in these acid-treated MWCNTs had a channel-like structure, as if a ring of material was cut away from the MWCNT around the circumference.

Of the 12 pristine MWCNTs tested here, 2 pristine MWCNTs became detached at one of the clamp sites during the tensile tests. No slippage or detachment was observed at the clamps during the tensile loading for the other 10 pristine, and for the 10 acid-treated, MWCNTs. The results from the successful tensile loading and breaking of 10 pristine and 10 acid-treated MWCNTs are thus reported here. A series of SEM images of an individual acid-treated MWCNT acquired before and after fracture are shown in Fig. 2.

An 11.13 ± 0.03 μm-long section of this MWCNT (Fig. 2a) was attached and then loaded and it fractured in the middle. The resulting fragment attached on the cantilever tip (Fig. 2b) had a length of at least 11.6 μm, whereas the other fragment on the W wire (Fig. 2c) had a length of at least 2.3 μm. Thus, the sum of the fragment lengths far exceeded the original section length. This apparent discrepancy can be explained as due to a 'sword-in-sheath'-type failure, similar to that observed in the failure mode of arc-discharge-grown MWCNTs and certain types of carbon fibers [15,28]. Similar 'sword-in-sheath' failure was observed in all 20 MWCNTs tested.

The cantilever (upper, Fig. 2a) was driven by the y linear picomotor of the tensile-loading stage and bent from the tensile load applied to the MWCNT linked between the cantilever tip and W wire (lower, Fig. 2a). By video recording the whole tensile test, both the deflection of the cantilever and the length change of the nanotube were simultaneously obtained. It has been reported that the transition from linear to nonlinear deformation of AFM cantilever occurs at the deflection of

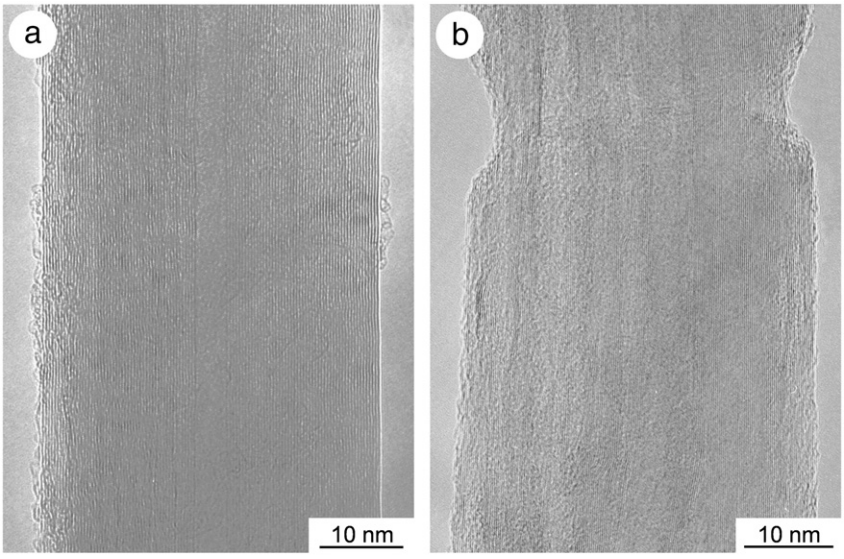

Fig. 1. TEM images of (a) a pristine and (b) an acid-treated MWCNTs that have nanoscale defects on their surfaces from the acid treatment.

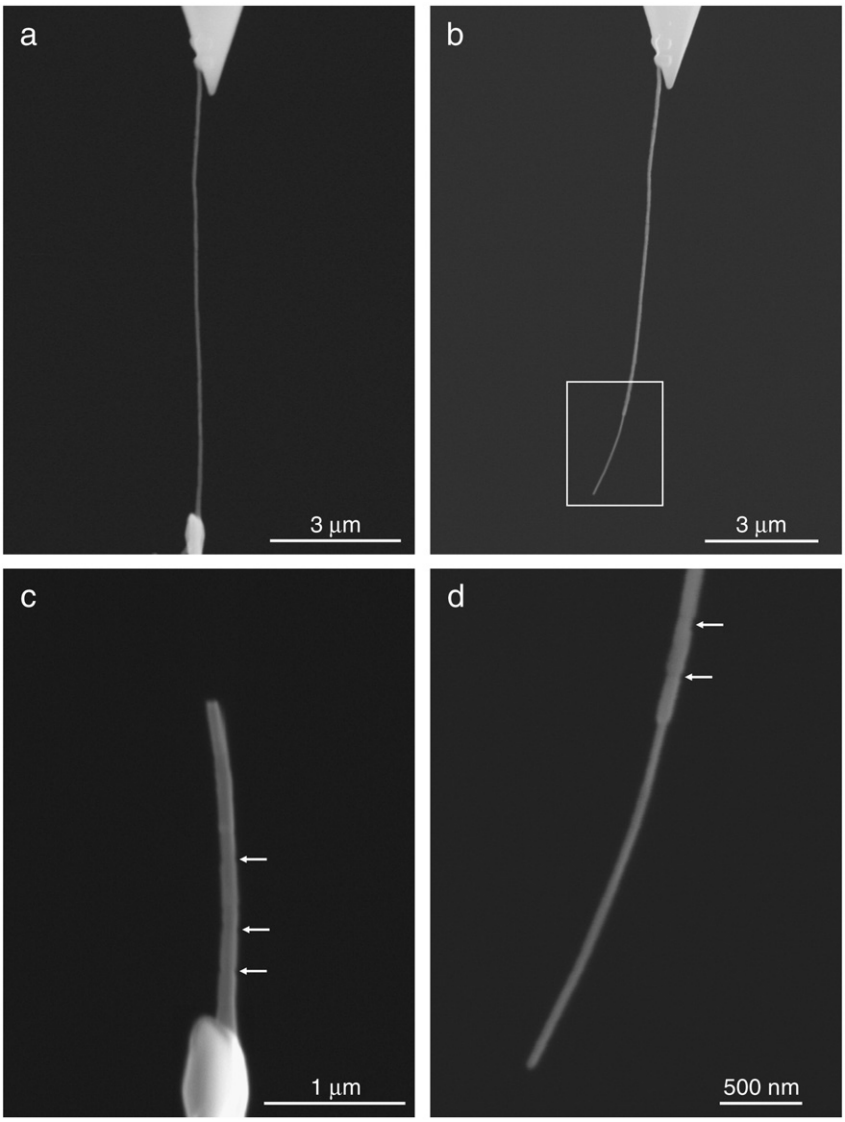

Fig. 2. Fracture of an acid-treated MWCNT captured in a series of SEM images. (a) An acid-treated MWCNT having a gauge length of 11.13 ± 0.03 μm before applying force. (b) After breaking, the fragment of the same MWCNT attached on the cantilever tip had a length of at least 11.6 μm. (c) The other fragment of the same MWCNT attached on the W wire had a length of at least 2.3 μm. (d) The high magnification image shows a 'sword-in-sheath'-type failure but with several changes in diameter clearly present along the fragment. The arrows in (c) and (d) indicate the position of the nanoscale defects.

cantilever tip (δ)/cantilever length (L) ratio of around 15% [29]. The largest deflection of 33.6 ± 1.9 μm (the force constant of cantilever was 0.27 N/m) was observed for the pristine MWCNT, and the cantilever length (L) emplyed this experiment was 326.86 ± 0.33 μm. Thus, the δ/L ratio of $10.3 \pm 0.6\%$ shows that Sader's method to calibrate the AFM cantilever is reliable. Fig. 3 shows the representative stress–strain curves in which stress was calculated from the effective cross-sectional area (S) of the MWCNT [$S = \pi(r_{\text{sheath}}^2 - r_{\text{sword}}^2)$, where r_{sheath} is the radius of the 'sheath' part and r_{sword} is the radius of the 'sword' part]. As seen in Fig. 3, the stiffness and fracture characteristics of the acid-treated MWCNTs are (on average) lower, due to the presence of the defects from the acid treatment. The measured tensile strengths of the pristine MWCNTs ranged from ~2 to ~48 GPa (mean 20 GPa) and for the acid-treated MWCNTs from ~1 to ~18 GPa (mean 6 GPa). The introduction of defects results in roughly a 70% decrease in mean tensile strength. The mean failure strain varied from 2.7% for the pristine MWCNTs to 1.9% for the acid-treated MWCNTs. The Young's modulus values obtained by a linear fit of each stress–strain curve ranged from ~50 to ~1360 GPa for the pristine MWCNTs and ~30 to ~1090 GPa for the acid-treated MWCNTs, respectively. For both types of MWCNTs

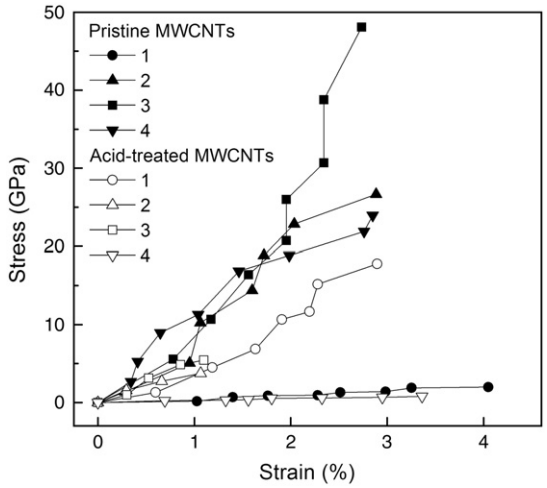

Fig. 3. Stress and strain curves of the pristine and acid-treated MWCNTs, where stress was calculated from the effective cross-sectional area of the broken MWCNTs (see text).

tested here, there was no apparent dependence of strength or Young's modulus on the MWCNT diameter or gauge length.

A comparison of the values reported here, with those of arc-discharge-grown MWCNTs where only the outer shell was evidently carrying the load, is relevant. The tensile strengths of 19 MWCNTs (outer-shell) values ranged from 11 to 63 GPa (mean 28 GPa) and the Young's modulus values of 4 MWCNTs ranged from 270 to 950 GPa [15]. It seems that the tensile strengths of the pristine MWCNT used in this research were somewhat lower than those of the arc-discharge-grown MWCNTs.

SEM images of the broken MWCNTs were evaluated to develop an understanding of the fracture mechanism. They are presented as examples of what happens as a result of loading to breaking. Of the 10 pristine MWCNTs tested here, 5 MWCNTs showed no apparent diameter change at the fractured region. As assumed by Yu et al. [15], we assume that the outer shell was carrying the load and the inner shells were not load-bearing. For the remaining 5 MWCNTs, however, the diameter of the broken MWCNTs was smaller at the fractured region, similar to the acid-treated MWCNT as shown in Fig. 2; perhaps significant inter-shell load transfer may be facilitated by the unique geometric structure arising from the CCVD synthesis and then high temperature annealing [20]. In particular, TEM images of the MWCNT powder reveal that there can be abrupt structural changes from perfect constant-diameter cylinders, such as pentagon and heptagon insertions and significant gaps between fringes. Similar observations have been made by others for this type of MWCNT [20]. Load transfer between layers is perhaps facilitated in some of these MWCNTs by the different structure and may be correlated to the unevenly spaced lattice fringes on one side of the hollow core.

SEM images of the fragments from all 10 acid-treated MWCNTs following fracture clearly indicate the involvement of more than the outer shell in the fracture event. By comparing the SEM images acquired before and after fracture, it was found that the fracture of the acid-treated MWCNTs clearly occurred at the channel-like defects in 8 out of 10 samples. In 6 samples there was a clear correlation that the location of a specific channel-like defect on the MWCNT prior to loading was where failure occurred. This indicates that the channel-like defects associated with the acid etching are typically going to be the weakest points in the acid-treated MWCNT structure and that stress concentration is present at the defect region; we also note that there may differences in the network of chemical bonds near such defects and if so, this might contribute as well.

4. Conclusions

In conclusion, tensile-loading experiments were performed on pristine MWCNTs having unusual internal structure and on their acid-treated analogs having channel-like defects of typically 10–20 nm depth. The mechanical properties of individual MWCNTs have been experimentally shown to strongly depend on their detailed structure and pronounced structural disorder can drastically reduce the mechanical properties. The measured tensile strength ranged from ~2 to ~48 GPa for the pristine MWCNTs, slightly lower than those of arc-discharge-grown MWCNTs [15]. For the acid-treated MWCNTs, measured strengths ranged from ~1 to ~18 GPa, which was roughly 70% lower than that of the pristine MWCNTs. Acid-treated MWCNTs having nanoscale defects have been effective in reinforcing structural ceramic components [7]. The results reported here suggest that the more effective interlocking of the 'notched' MWCNTs (from acid treatment), in the composites, more than offsets the reduction in tensile strength of acid-treated vs. pristine MWCNTs of this type.

Acknowledgments

The work was supported by a Grant-in-Aid from the Japan Society for the Promotion of Science (JSPS) Fellows for GY's 6-month visit to the Ruoff group. Ruoff group members (JWS, JHA, RDP, and RSR) were supported by the NSF #0802247, Fracture Mechanics of Nanowires and Nanostructures, D. Kouris program manager, and the DARPA N/MEMS S&T Fundamentals Program, D. Polla program manager. The authors thank M. Miyazaki of Technical Division, School of Engineering, Tohoku University, for his technical assistance in the TEM analysis.

References

[1] A.A. Mamedov, N.A. Kotov, M. Prato, D.M. Guldi, J.P. Wicksted, A. Hirsch, Nat. Mater. 1 (2002) 190.
[2] G.D. Zhan, J.D. Kuntz, J. Wan, A.K. Mukherjee, Nat. Mater. 2 (2002) 38.
[3] X. Wang, N.P. Padture, H. Tanaka, Nat. Mater. 3 (2004) 539.
[4] G. Yamamoto, Y. Sato, T. Takahashi, M. Omori, T. Hashida, A. Okubo, K. Tohji, J. Mater. Res. 21 (2006) 1537.
[5] G. Yamamoto, Y. Sato, T. Takahashi, M. Omori, A. Okubo, K. Tohji, T. Hashida, Scripta Mater. 54 (2006) 299.
[6] N. Hu, Z. Masuda, C. Yan, G. Yamamoto, H. Fukunaga, T. Hashida, Nanotechnology 19 (2008) 215701.
[7] G. Yamamoto, M. Omori, T. Hashida, H. Kimura, Nanotechnology 19 (2008) 315708.
[8] G. Yamamoto, M. Omori, K. Yokomizo, T. Hashida, K. Adachi, Mater. Sci. Eng. B 148 (2008) 265.
[9] E. Hernandez, C. Goze, P. Bernier, A. Rubio, Phys. Rev. Lett. 80 (1998) 4502.
[10] T. Ozaki, Y. Iwasa, T. Mitani, Phys. Rev. Lett. 84 (2000) 1712.
[11] T. Dumitrica, T. Belytschko, B.I. Yakobson, J. Chem. Phys. 118 (2003) 9485.
[12] S. Ogata, Y. Shibutani, Phys. Rev. B 68 (2003) 165409.
[13] D. Troya, S.L. Mielke, G.C. Schatz, Chem. Phys. Lett. 382 (2003) 133.
[14] S.L. Mielke, D. Troya, S. Zhang, J.L. Li, S.P. Xiao, R. Car, R.S. Ruoff, G.C. Schatz, T. Belytschko, Chem. Phys. Lett. 390 (2004) 413.
[15] M.F. Yu, O. Lourie, M.J. Dyer, K. Moloni, T.F. Kelly, R.S. Ruoff, Science 287 (2000) 637.
[16] A.H. Barber, R. Andrews, L.S. Schadler, H.D. Wagner, Appl. Phys. Lett. 87 (2005) 203106.
[17] A.H. Barber, I. Kaplan-Ashiri, S.R. Cohen, R. Tenne, H.D. Wagner, Compos. Sci. Technol. 65 (2005) 2380.
[18] W. Ding, L. Calabri, K.M. Kohlhaas, X. Chen, D.A. Dikin, R.S. Ruoff, Exp. Mech. 47 (2007) 25.
[19] B. Peng, M. Locascio, P. Zapol, S. Li, S.L. Mielke, G.C. Schatz, H.D. Espinosa, Nat. Nanotechnol. 3 (2008) 626.
[20] Y.A. Kim, T. Hayashi, M. Endo, Y. Kaburagi, T. Tsukada, J. Shan, K. Osato, S. Tsuruoka, Carbon 43 (2005) 2243.
[21] J. Chen, J.Y. Shan, T. Tsukada, F. Munekane, A. Kuno, M. Matsuo, T. Hayashi, Y.A. Kim, M. Endo, Carbon 45 (2007) 274.
[22] J.P. Salvetat, A.J. Kulik, J.M. Bonard, G.A.D. Briggs, T. Stockli, K. Metenier, S. Bonnamy, F. Beguin, N.A. Burnham, L. Forro, Adv. Mater. 11 (1999) 161.
[23] S.L. Mielke, S. Zhang, R. Khare, R.S. Ruoff, T. Belytschko, G.C. Schatz, Chem. Phys. Lett. 446 (2007) 128.
[24] W.Q. Ding, L. Calabri, X.Q. Chen, K.M. Kohhaas, R.S. Ruoff, Compos. Sci. Technol. 66 (2006) 1112.
[25] W. Ding, D.A. Dikin, X. Chen, R.D. Piner, R.S. Ruoff, E. Zussman, X. Wang, X. Li, J. Appl. Phys. 98 (2005) 014905.
[26] J.E. Sader, J.W.M. Chon, P. Mulvaney, Rev. Sci. Instrum. 70 (1999) 3967.
[27] J.E. Sader, I. Larson, P. Mulvaney, L.R. White, Rev. Sci. Instrum. 66 (1995) 3789.
[28] G.G. Tibbetts, C.P. Beetz, J. Phys. D-Appl. Phys. 20 (1987) 292.
[29] W. Ding, Z. Guo, R.S. Ruoff, J. Appl. Phys. 101 (2007) 034316.